RESEARCH ARTICLE           OPEN ACCESS

# Power Quality Improvement of an Off-Grid Versatile PV System

## D. Bini Sherlin[*], J.C. Paul Immanuel[**]
[*] (PG Scholar, Department of EEE, DMI College of Engineering, Chennai, India)
[**] (Assistant Professor, Department of EEE, DMI College of Engineering, Chennai, India)

**ABSTRACT**
Photovoltaic systems are trusted to be the future wave of alternate source of energy. This paper presents a versatile PV generation system that enables to supply both AC as well as DC loads in addition to providing back-up supply for the AC load. The back-up supply is provided by charging a battery. The inverter is controlled using hysteresis current control method that contains the current ripple within the two hysteresis bands. Thereby the harmonic content in the inverter output is lowered and also provides quality power. The performance of the proposed system is verified through simulation.
*Keywords* – Photo Voltaic (PV), Maximum Power Point Tracking (MPPT), Converter, Inverter, Current Control

## I. INTRODUCTION

The rising need for sustainable energy development due to the fast depleting fossil fuels have lead to the use of efficient alternate sources of energy. Solar PV systems are widely preferred and also area of research in recent times.

Maximum performance is obtained from PV panel by using MPPT algorithms. Comparative surveys and evaluations are presented in [1] – [3]. Among the many MPPT algorithms the *Perturbation and Observation* (P&O) is the simplest and also commonly used algorithm. To identify the suitable duty ratio in which the DC-DC converter should be operated to maximize the power output, the P&O MPPT algorithm was used in [4]. The results proved that the photo voltaic array with proposed MPPT controller could operate in the maximum power point for the whole range of assumed solar data (irradiance and temperature). A simulation study of MPPT for photovoltaic systems using perturb and observe algorithm is presented in [5].

A family of single-inductor multiple-output switching converters that provided both positive and negative output voltages was proposed in [6]. With time multiplexing control, both step-up and step-down bipolar outputs were achieved. Compared to conventional converters, the number of inductors and power devices are reduced significantly. A new DC–DC *multi-output boost* (MOB) converter which could share its total output between different series of output voltages for low- and high-power applications is presented in [7].

The concept of an impedance-source (or impedance-fed) power converter (abbreviated as Z-source converter) is presented in [8]. The Z-source converter employs a unique impedance network (or circuit) to couple the converter main circuit to the power source. [9] extends the impedance-source (Z-source) inverters concept to the transformer-based Z-source (trans Z-source) inverters followed by voltage-type Γ-Z-source inverters that used a unique Γ-shaped impedance network for boosting their output voltage in addition to their usual voltage buck behavior are proposed in [10].

A hysteresis current controller which combines the advantages of both symmetrical unipolar PWM and hysteresis techniques is presented in [11]. Various hysteresis modulation approaches available in the literature for multilevel converters is given in [12]. The pros and cons of various techniques are described and compared for tracking the reference signal in order to attain an adequate switching optimization, excellent dynamic responses and high accuracy in steady-state operation.
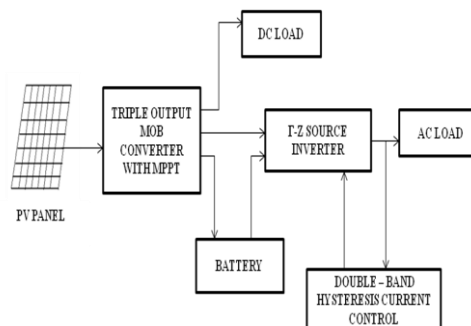
## II. PROPOSED SYSTEM



Fig. 1 Proposed System Block Diagram

The proposed system comprises of a PV panel that is connected to the MOB converter which boosts the input. The MOB converter is controlled

using P&O MPPT technique thereby providing maximum obtaining maximum power from the solar panel. The MOB converter provides three outputs. First output charges a battery and second output is used for supplying DC load. The third output is given to an inverter that inverts the input DC supply and supplies the AC load. The current ripple of the inverter is contained within limits using hysteresis current controller that gives fast response. The harmonic content of the inverter output is also thus lowered. Fig. 1 shows the block diagram of the proposed system.

### III. BOOST CONVERTER

A single inductor multi-output boost (MOB) converter with series regulated output voltages is utilized in this paper. The use of a single inductor reduces the number of external bulky components such as inductors and power switches, leading to decreased cost and losses in the system.

The converter circuit consists of a boost switch M, 2 sharing switches M1 and M2, 3 diodes ($D_1$ to $D_3$), an inductor and 3 capacitors ($C_1$ to $C_3$) with different loads ($R_1$ to $R_3$). $D_1$ to $D_3$ are used to block the negative voltage and provide two quadrant operation of $S_1$ to $S_2$. The inductor L is used for current limiting purposes. The circuit of proposed inverter is shown in fig. 2.
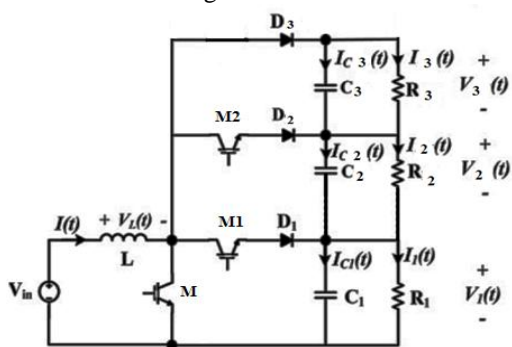


Fig. 2 MOB Converter Circuit

### 3.1 Operation of MOB converter

In the subinterval zero, switch M is turned 'on' and the inductor is charged by the current flowing through it. In the following N subintervals, M remains 'off' and the M1, M2 are switched to charge the two capacitors into the desired value. When M1, M2 are 'off', the diode ($D_3$) directs the inductor current to charge all $C_1$ to $C_3$ to generate $V_1$ to $V_3$, respectively.

Table 1. Switches M, M1, M2 Switching States

| Switching states | M | M1M2 | $C_1$ | $C_2C_3$ |
|---|---|---|---|---|
| 10 | On | Off | Discharge | Discharge |
| 01 | Off | On | Charge | Discharge |
| 00 | Off | Off | Charge | Charge |

In MOB converter there are three possible switching states as switches M1M2 cannot be turned 'on' while M is 'on'. The switching states of the MOB converter are shown in the table 1. The inductor current and switching signals waveform is shown in figure 3. $D_1$ is the duty cycle of switches M1M2 and $D_0$ is the duty cycle of switch M.
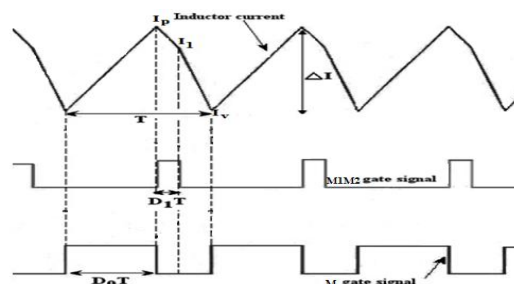


Fig. 3 Inductor Current and Gating Signals of Proposed MOB Converter

### 3.2 Gate Pulse Generation

P&O MPPT technique is used for generation of the gate pulse for the main boost switch M. P&O is the most commonly used algorithm in MPPT algorithms because of its simplicity. Perturbation and Observation tracks the Maximum Power Point (MPP) all the time, irrespective of the atmospheric conditions, type of PV panel, and even aging, by processing actual values of PV voltage and current. They operate by periodically perturbing (i.e. incrementing or decrementing) the array termed voltage and comparing the PV output power with that of the previous perturbation cycle. If the power is increasing, the perturbation will continue in the same direction in the next cycle, otherwise the perturbation direction will be reversed. This means the array terminal voltage is perturbed every MPPT cycle. The duty cycle is adjusted accordingly. The other two switches M1 and M2 are triggered through pulse generators.

### 3.3 Steady State Equations

The total time period T is given by:

$$T = T_{10} + T_{01} + T_{00} \qquad (1)$$

The average inductor voltage over one cycle should be zero.

$$T_{10}(V_{in}) + T_{00}(V_{in} - V_1 - V_2 - V_3) + T_{01}(V_{in} - V_1 - V_2) = 0 \qquad (2)$$

where $T_{00}$ = Time interval during which all switches are turned OFF, $T_{10}$ = Time interval during which only switch M is turned ON, $T_{01}$ = Time interval during which switches M1 and M2 are turned ON and M is turned OFF, T = Total switching period, $V_{in}$ = Input source voltage. $V_1$, $V_2$, $V_3$ = Output voltages of MOB converter.

### 3.4 Dynamic State Equations

*Mode 1: When switch M is ON and switches M1, M2 are OFF at instant $T_{10}$*

$$T_{10} = \Delta I \div (V_{in} - L\frac{dI}{dT})  \tag{3}$$

where L = Inductance of MOB converter, $\Delta I$ = Change in inductor current, $I_p$ = Maximum value of inductor current, $I_v$ = Minimum value of inductor current.

*Mode 2: When switch M is OFF and switches M1, M2 are ON at instant $T_{01}$*

$$T_{10} = (I_1 - I_P) \div \left[\frac{1}{L}\int V_{in}dt - C\left(2\frac{dV_0}{dt}\right) + \frac{3}{R}V_0\right]  \tag{4}$$

where $V_0 = V_1 = V_2 = V_3$ , $R = R_1 = R_2 = R_3$ and $C = C_1 = C_2 = C_3$, $V_0$ = Output voltage of MOB converter, R = Equivalent resistance of MOB converter, C = Equivalent capacitance of MOB converter, $I_1$ = Intermittent value of inductor current before falling to $I_v$.

*Mode 3: When switch M is OFF and switches M1, M2 is OFF at instant $T_{00}$*

$$T_{00} = (I_V - I_1) \div \left(V_{in} - L\frac{dI}{dt} - V_0\right)  \tag{5}$$

## IV. □-Z SOURCE INVERTER

The inverter used in the proposed system is Γ-Z source inverter. The third output from the MOB converter is given as input to the inverter. The inverter converts the DC input to AC output to feed AC loads.

This paper employs a single phase inverter with equally coupled inductors and single capacitor as shown in fig. 4. The source is connected to the two coupled inductors $W_1$ and $W_2$. $W_2$ is connected in series to the DC link capacitor C. The diode $D_{\Gamma Z}$ is used for its reverse blocking capability which prevents high current from flowing to the source under shoot-through state.
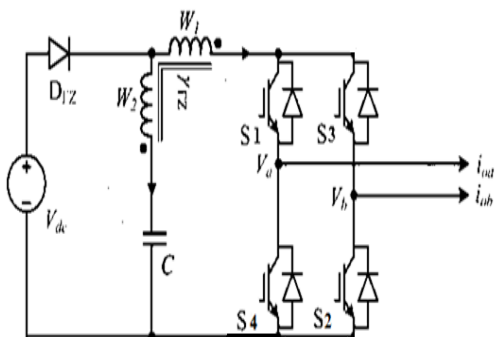


Fig. 4 Γ-Z Source Inverter Used in Proposed System

The voltage boosted by the coupled inductors and DC link is applied to the inverter bridge. Switches $S_1$ and $S_2$ are fired together while $S_3$ and $S_4$ are fired 180° after $S_1$ and $S_2$. Neither $S_1S_3$ nor $S_2S_4$ can conduct simultaneously. For example whenever $S_3$ and $S_4$ are in the forward blocking state and a gate pulse is applied to them, they turn ON and at the same time a negative voltage is applied across $S_1$ and $S_2$ commutating them immediately. Therefore, the only possible conduction modes when the current $i_0$ flows are $S_1S_2$ and $S_3S_4$ where $i_0$ is the load current.

## V. CURRENT CONTROL OF INVERTER

A single-phase full-bridge inverter is shown in fig. 5. $E_d$ is the input source. 'u' and 'v' are the output terminals. R, L, $e_0$ represents the RLE load connected to the inverter. $i_0$ represents the load current flowing through the load connected to the inverter.
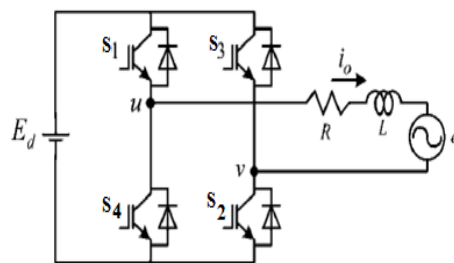


Fig. 5 Single-Phase Full Bridge Inverter

An inner current controller is usually used to control the output current of the inverter for improving the performance. A hysteresis current controller is commonly used here because of its simplicity and robust nature against various disturbances. Also, besides fast response current loop, the method does not need any knowledge of load parameters. In this paper, the single band current hysteresis control is used. The reference signal is a sine wave of amplitude 0.2.

### 5.1 Double-Band Hysteresis Current Control

The scheme of this controller is shown in fig. 6. In this controller, one pair of switches (e.g. $S_1$ and $S_2$) is controlled by the smaller hysteresis band and another pair of switches ($S_3$ and $S_4$) is controlled by the larger hysteresis band. Because the hysteresis band is different, the output current error is mainly determined by the smaller hysteresis band.

The larger hysteresis band is active only when the smaller hysteresis band has lost the ability to control the current error. The smaller hysteresis band cannot control the current error when the average output voltage polarity is reversed. When this condition occurs, the larger hysteresis band will become active to change the polarity of the output voltage. Thus, the pair of switching devices that is controlled by the larger hysteresis band is switched at the fundamental output frequency.

During the positive half-cycle of the output voltage, switch $S_4$ (switch $S_3$) receives an ON signal (OFF signal). On the other hand, during the negative half-cycle of the output voltage, switch $S_4$ (switch $S_3$) receives an OFF signal (ON signal). The output current error is controlled by switches $S_1$ and $S_2$. The output voltage has a unipolar characteristic similar to asymmetrical unipolar carrier-based PWM.
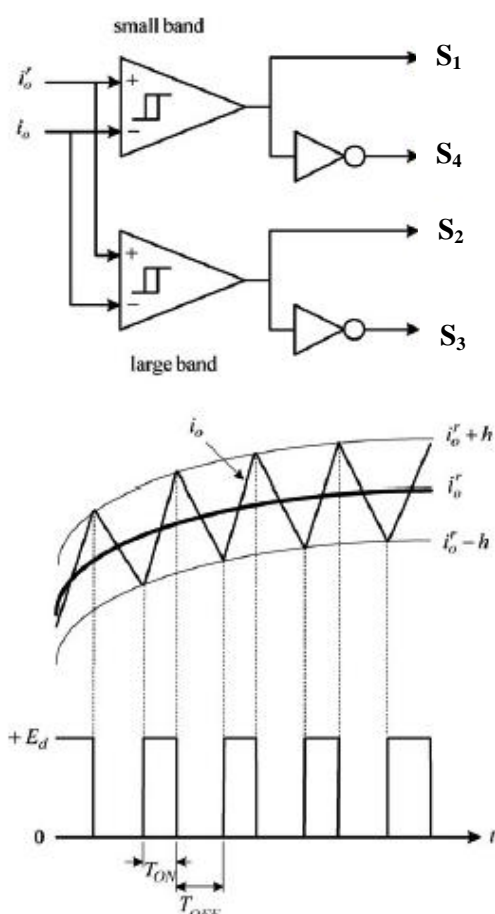




Fig. 6  Double Band Hysteresis Current Control

## VI. PROPOSED SYSTEM SIMULATION

The simulation of the proposed system with hysteresis current control is carried out in MATLAB and shown in fig. 7. It combines the simulation of solar panel, MPPT, MOB converter, Γ-Z source inverter and hysteresis current controller.

The solar panel block is wrapped in a subsystem whose voltage and current outputs are obtained. The voltage terminal is connected to the controlled voltage source that connects the solar panel to the MOB converter. The current output of solar panel is connected to the MPPT block that generates gating signals for the main boost switch M of the MOB converter. The voltage boosted by the main switch is shared by the switches M1 and M2. The switches M1 and M2 are triggered by pulses from

pulse generators PG1 and PG2 respectively. The MOB converter boosts the input and provides three outputs.
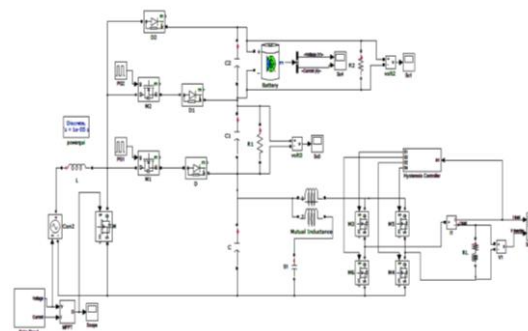


Fig. 7 Simulation of Proposed System

The first output is connected to a battery. The battery gets charged using the MOB converter output and discharges through a resistor. The second output is connected to a resistive load. The third output is connected to the Γ-Z source inverter that feeds an R-L load predominantly inductive. The inverter is connected to the MOB converter at the terminals of capacitor C. The inverter converts the input DC to Ac output. The actual current from the inverter is measured using current measurement block and given to hysteresis current controller block as input which compares it with reference sine wave and generates switching pulses for the inverter switches.

## VII.    SIMULATION RESULTS

The solar panel consists of 36 solar cells with irradiation value 150. The panel produces 15 volts output with 1 ampere current. The output power produced is about 15.5 watts as shown in fig. 8.
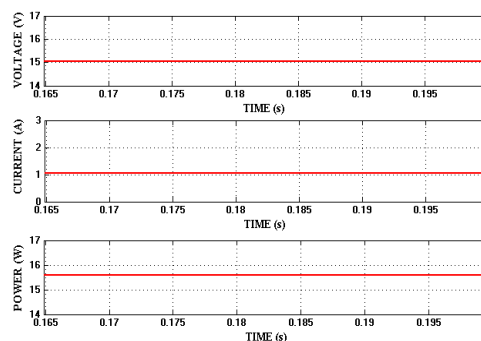


Fig. 8 Solar panel Output

The MOB converter produces three outputs of which one is used for battery charging. The battery is used as back-up supply for the inverter. The nominal value of the battery is set and simulated. The voltage output and current output during battery charging is shown in fig. 9. As seen from the output, the battery charged voltage is approximately 45 volts. The current is nearly zero since the voltage is highest when charging.
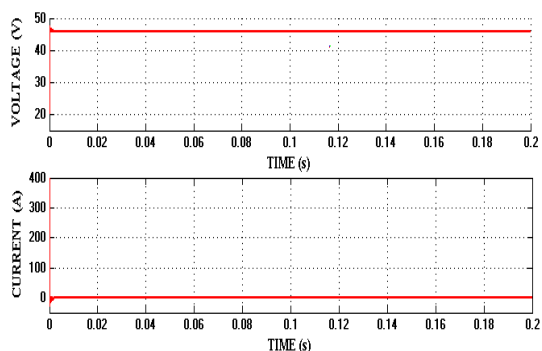
Fig. 9 Charging of Battery

The battery discharges through a resistor connected to its terminals. The battery voltage reduces as the battery discharges during simulation. The output voltage during battery discharge is shown in fig. 10. There is a nearly 0.06 volt drop when simulated for 10 seconds.
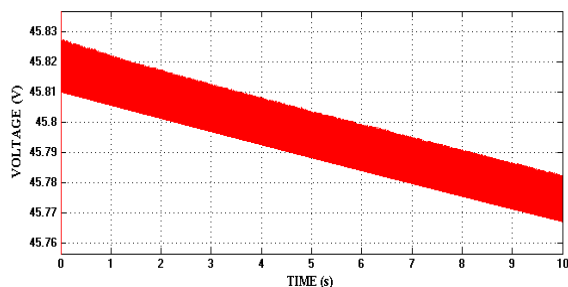

Fig. 10 Battery Discharging

The MOB converter produces three outputs. All the three outputs are of equal magnitude. As seen from the output, the each output measures nearly 45 volts. The voltage value rises in the beginning of the simulation and remains constant throughout the simulation. The output is shown in fig. 11.
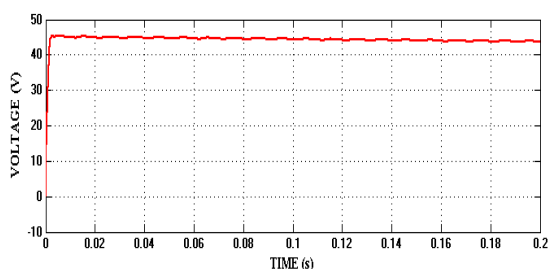

Fig. 11 Output of MOB Converter

The simulated output of the Γ-Z source inverter is shown in fig 12. The actual current is given to the hysteresis current controller block. The current is limited between the hysteresis bands. The load current and the inverter voltage are shown in the output. The load current is 0.2 amperes and inverter voltage is nearly 45 volts.
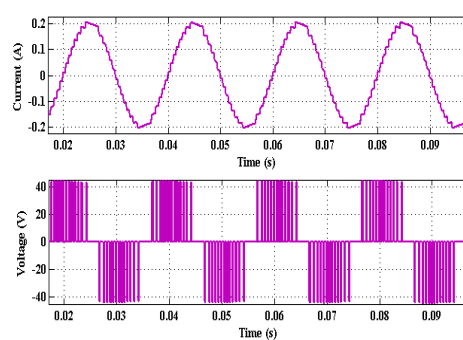

Fig. 12 Inverter Output

To visualize the load current tracking the reference wave within the hysteresis bands, the reference current wave and the inverter load current wave are multiplexed using a multiplexer block inside the hysteresis current controller block and is shown in fig. 13. The reference wave is set at 0.2 amplitude and 50 Hz frequency. It is shown by blue colour line. The actual load current is shown by red colour.
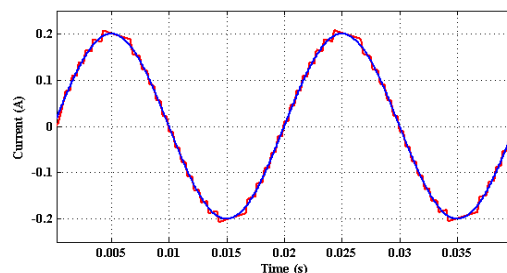

Fig. 13 Inverter Current Tracking reference wave

The THD analysis of the proposed system with single - band hysteresis current control method is shown in fig. 14. The FFT analysis is performed for one cycle at 50 Hz frequency. The THD content after FFT analysis was found to be 4.80%.
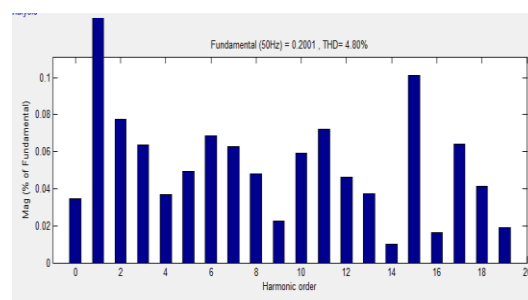

Fig. 14 THD Analysis of Proposed System with Single-band Hysteresis Current Control

The fig. 15 shows the THD analysis of the proposed system with double – band hysteresis current control. There is drastic change in the shape of the waveform. The analysis was done for one cycle and with 50 Hz frequency. The THD content

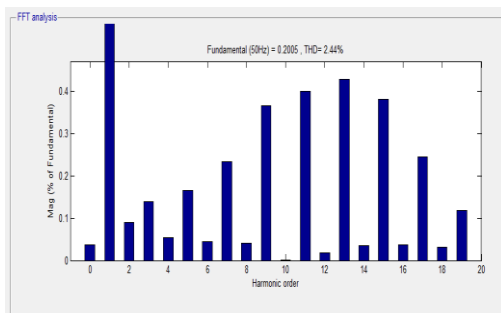was found to be 2.80% which is very less compared to the previous analysis.



Fig. 15 THD Analysis of Proposed System with Double-band Hysteresis Current Control

## VIII. CONCLUSION

This paper presents a versatile PV generation system along with battery charging that provides supply to both AC as well as DC loads. With the use of MPPT technique**,** maximum power is obtained from the solar panel thereby increasing the efficiency of the solar panel. The paper implements a triple output MOB converter that shares equal voltages of 45 volts in all the three output terminals. The inverter used for conversion of DC to AC for supplying AC loads uses only two coupled inductors and a capacitor for voltage boosting. Hence inverter rating and component count are greatly reduced. Further the paper uses a simple yet fast responding hysteresis current control method that contains the current ripple within the hysteresis bands and also reduces the harmonics as seen from the simulation results. The average value of inverter current also gets reduced to 0.038 amperes and this control method provides overcurrent protection of the inverter and connected load as well. The presence of battery backup of 45 volts extends the operation of inverter circuit when the solar input is minimal. Thus this paper presents an economic as well as an efficient off-grid PV generation system.

## REFERENCES

[1] S. Jain and V. Agarwal "Comparison of the performance of maximum power point tracking schemes applied to single-stage grid-connected photovoltaic systems" in *IET Electr. Power Appl.*,vol. 1, no. 5, pp. 753–762, Sep. 2007.

[2] M. A. G. de Brito, L. Galotto. Jr., L. P. Sampaio, G. A. Melo, and C. A. Canesin "Evaluation of the Main MPPT Techniques for Photovoltaic Applications" in *IEEE Trans on Industrial Electronics,* vol. 60, no. 3, pp. 1156-1167, March 2013.

[3] R. Faranda, S. Leva and V. Maugeri "MPPT techniques for PV Systems: energetic and cost comparison" in *IEEE PESGMCDEE'08*, pp.1-6 Jul. 2008.

[4] R.Sridhar, S.Jeevananthan, N.Thamizh Selvan and Sujith Chowdary "Performance Improvement of a Photo Voltaic Array Using MPPT (P&O) Technique" in *IEEE ICCCCT'10*, pp. 191-195, Oct. 2010.

[5] S. Alsadi and B. Alsayid "Maximum Power Point Tracking Simulation for Photovoltaic Systems Using Perturb and Observe Algorithm" in *IJEIT* vol. 2, Iss. 6, pp. 80-85, Dec. 2012.

[6] D. Ma and W. H. Ki "Single-inductor multiple output switching converters," in *Proc. IEEE PESC'01*, pp. 236-231, May 2001.

[7] A. Ghosh, A. Nami, F. Blaabjerg, and F. Zare "Multi-Output DC–DC Converters Based On Diode-Clamped Converters Configuration : Topology And Control Strategy" in *IET Power Electron.*, vol. 3, Iss. 2, pp. 197–208, March 2010.

[8] F. Z. Peng "Z-source inverter," in *IEEE Trans. Ind. Appl.*, vol. 39, no. 2,pp. 504–510, Mar./Apr. 2003.

[9] F. Z. Peng, H. Cha and W. Qian "Trans-Z-source inverters," in *IEEE Trans. Power Electron*., vol. 26, no. 12, pp. 3453–3463, Dec. 2011.

[10] D. Li, F. Blaabjerg, and P. Chiang Loh "T-Z-Source Inverters," in *IEEE Trans. Power Electron.,* vol.28, no.11, pp. 4880-4884, Nov. 2013.

[11] P.A. Dahono "New hysteresis current controller for single-phase full-bridge inverters," in *IET Power Electron.*, vol. 2, Iss. 5, pp. 585–59, Sep. 2009.

[12] A. Ghosh, A. Joshi and A. Shukla "Hysteresis Modulation of Multilevel Inverters," in *IEEE Trans. on Power Electronics*, vol. 26, No. 5, pp. 1396-1409, May 2011.